Original paper

Solvothermal Synthesis of Reduced Graphene Oxide as Electrode Material for Supercapacitor Application

Mohammad R. Thalji [a], Gomaa A. M. Ali [b], Soon Poh Lee [a], Kwok Feng Chong [a, *]

[a] Faculty of Industrial Sciences & Technology, Universiti Malaysia Pahang, Gambang, 26300 Kuantan, Malaysia
[b] Chemistry Department, Faculty of Science, Al–Azhar University, Assiut, 71524, Egypt

Abstract

This work manifests the synthesis of reduced graphene oxide nanosheets through *in situ* solvothermal reduction of graphene oxide. The as-synthesized reduced graphene oxide nanosheets are utilized as a supercapacitor electrode. A series of structural and morphological investigations evince that graphene oxide can be successfully reduced through solvothermal strategy in absolute ethanol as solvent. Fourier transform infrared spectroscopy results showed that reduced graphene oxide displayed very low-intensity bands related to oxygenated functional groups, implying a high reduction degree. Besides that, it shows good electrochemical characteristics such as high specific capacitance of 183 F g^{-1} is obtained in 5 M KOH at 0.25 A g^{-1} and low internal and charges transfer resistances which are 430 and 64 mΩ, respectively. The findings confirm that graphene oxide can be reduced through solvothermal reduction strategy. Further, the as-prepared reduced graphene oxide nanosheets is a good candidate for supercapacitors application.

1. Introduction

As a result of high consumption of non-renewable energy resources, the improvement of various energy storage devices becomes urgently necessary [1–3]. Electrochemical capacitors, also are known as supercapacitors, represent an important class of energy storage systems [4, 5]. They have attracted broad interest due to their outstanding features like high power density, fast charging-discharging, and superior long-term

stability [6, 7]. In contrast, they suffer relatively from low energy density. Typically, supercapacitor can be divided into two main types: electric double-layer capacitors (EDLCs) and pseudocapacitors [8]. The EDLC uses the charges accumulated on the interfacial electrolyte/electrode surface, which principally includes the carbon-based materials with a high specific surface area [9]. While the latter employs metal oxides, metal hydroxides or conductive polymers as an electrode material, which means a faradaic mechanism to store charges [10, 11]. However, several two-dimensional (2D) nanomaterials were evolved which employed as electrodes in energy storage devices. These nanomaterials provide wide characteristics such as increases the specific surface area and reduce the ion diffusion distance. Furthermore, they can improve the access of electrolyte to as many active materials sites as possible and improve the ion diffusion kinetics [12]. Graphene considers as an ideal 2D material for the energy storage field due to its high surface area, excellent electrical conductivity and chemical stability [13–15]. Till now, several methods have been reported on fabrication of the graphene such as chemical vapor deposition, epitaxial growth, hydrothermal/solvothermal synthesis, micromechanical exfoliation of graphite and the reduction of graphene oxide (GO) [16–19]. Generally, the chemical reduction of GO using a strong reducing agent, such as hydrazine, is a dangerous and toxic approach, and it is usually determined the quality degree of graphene [20]. By the solvothermal reduction strategy, some reports found that GO dispersion can be reduced to graphene nanosheets in various solvents, such as ethanol, ethylene glycol, N-Methyl-2-Pyrrolidone (NMP), 1- butanol and N, N-dimethylformamide (DMF) [21, 22].

Therefore, in this work, we demonstrate the preparation of reduced graphene oxide (rGO) nanosheets using solvothermal reduction of GO. First, the graphite oxide was prepared using the modified Hummers' method. Then, rGO was obtained using solvothermally in absolute ethanol as a reductant solvent. Finally, the as-prepared rGO is studied by X-ray diffraction (XRD), Fourier transform infrared spectroscopy (FTIR) and field emission scanning electron microscopy (FESEM). The as-prepared rGO is applied to the preparation of the supercapacitor electrode.

2. Experimental

2.1 Material synthesis

Graphene oxide (GO) was synthesized through modified Hummers' method using graphite flake (+100 mesh, Graphene Supermarket) [23, 24]. rGO was prepared *via* the following procedure, first, graphite flake (4 g) was put into a mixture of concentration H_2SO_4 (30 mL), $K_2S_2O_8$ (6 g) and P_2O_5 (6 g). The solution was heated to 80 °C and kept stirring for 6 h by using oil-bath. Next, the mixture was cooled to room temperature and diluted with deionized water (2 L) overnight. The product was obtained by filtering using Whatman filter paper and dried naturally. The pre-oxidized graphite was then reoxidized by modified Hummers' method. Pre-treated graphite powder was put into 0 °C concentrated H_2SO_4 (300 mL). Then, $KMnO_4$ (35 g) was added gradually under stirring and the temperature of the mixture was kept being below 20 °C by ice bath. Successively, the mixture was stirred at 35 °C for 4 h and then diluted with deionized water (900 mL). The mixture was stirred at 55 °C for 20 min. 100 mL 30% H_2O_2 drop by drop. The mixture was filtered and washed with 1:10 HCl aqueous solution (2 L) followed by deionized water. The resulting solid was dried. Exfoliation was carried

out by sonicating graphite oxide dispersion in absolute ethanol (1.2 mg mL^{-1}) for 4 h. Reduction is then carried out by adding hydrazine monohydrate (1.2 mL) into GO solution. Afterwards, the mixture was transferred into a Teflon-lined autoclave which was heated at 200 °C for 10 h. A black precipitate was finally collected and washed repeatedly with absolute ethanol and water, followed by vacuum drying at 80 °C overnight.

2.2 Characterization methods

The crystal structure of as-synthesized materials was determined by XRD (Rigaku Miniflex II, Japan), equipped with an automatic divergent slit (Cu-Kα radiation, λ = 0.15418 nm) in the diffraction range from 8 to 80°. Fourier transform infrared spectroscopy (FTIR) spectra were recorded on using PerkinElmer Spectrum 100 spectrophotometer in the range 400-4000 cm^{-1} with 2 cm^{-1} resolution using the KBr pellet technique (1 mg sample in 100 mg KBr). The morphology of the sample was investigated through a field emission scanning electron microscope (FESEM, JEOL JSM-7800F, USA) operating at 30.0 kV.

2.3 Electrochemical characterization

Cyclic voltammetry (CV), galvanostatic charge-discharge (GCD) and electrochemical impedance spectroscopy (EIS) measurements were conducted using a potentiostat-galvanostat (PGSTAT M101, Metrohm Autolab B.V.) in 5 M KOH aqueous electrolyte. The EIS determination was carried out in the frequency range of 10^{-2} Hz to 100 kHz to determine the electrical resistance and prove the capacitive performances of the rGO electrode at the open circuit voltage. The working electrode was prepared by mixing 90 wt.% of as-

prepared rGO, 5 wt.% carbon black and 5 wt.% polytetrafluoroethylene (PVDF). Then, the homogeneous slurry was coated on nickel foam substrate (~1 cm^2), then pressed at a pressure of 10 MPa and dried at 70 °C for 24 h. Finally, the mass loading of active material in the working electrode was ca. 4 mg. Electrochemical performances of the rGO electrode were evaluated in three-electrode system, where, rGO electrode was used as working electrode, Pt wire and Ag/AgCl were used as counter and reference electrodes, respectively. The specific capacitance values (Csp, F g^{-1}) at different current densities were calculated based on the discharge curves using the formula $C = It/(m \Delta V)$ [25, 26], where I, t, ΔV and m are the charge-discharge current (A), discharge time (s), total potential deviation (V), and the mass of electrode material (g), respectively.

3. Results and Discussion

3.1 Structural and morphological characterization

The XRD patterns of all samples including graphite flakes, GO and rGO are shown in Figure 1. As seen, the XRD pattern of graphite flake displayed a strong and sharp peak (002) at 2θ = 26.6° and it was disappeared after the oxidation. For GO samples, typical (001) peak at about 11.3° is observed, exhibiting similar crystalline structure of previously reported [27]. On the other hand, the oxygen-containing functional groups in GO couldn't be completely got rid of through solvothermal reduction method. A broad peak of graphite (002) at approximately 24.5° still remained in the XRD pattern of rGO nanosheets. In general, the diffraction peak of graphite flakes is very strong and sharp, while the diffraction peak of rGO is relatively weak and blunt, indicating their ultra-thin sheets [28, 29].
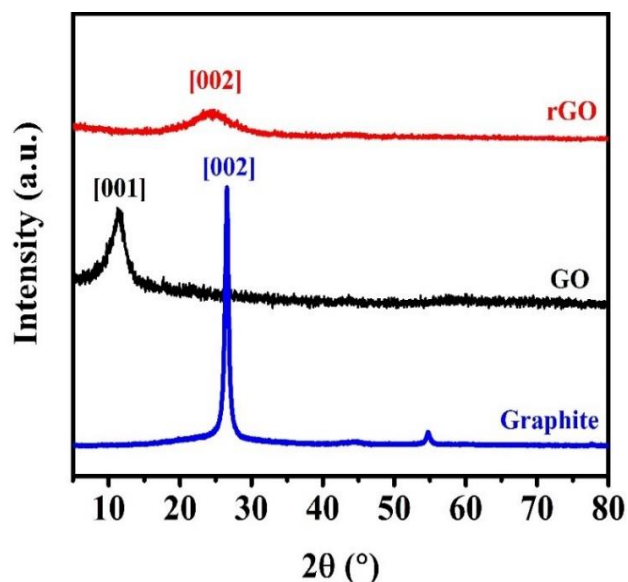
Figure 1: XRD patterns of graphite, GO and rGO nanosheets.

Figure 2: FTIR spectra for GO and rGO nanosheets.

Figure 2 shows the FTIR spectra of GO and rGO nanosheets. The GO spectrum displays peaks at 3445, 1732, 1628, 1384, 1240 and 1080 cm^{-1} which belong to O–H vibration, C=O carbonyl stretching, stretching of C=C alkene group, C–OH, C–O–C and C–O, respectively [30]. The high intensity peaks reveal that large amount of oxygen containing groups are present after oxidation process. After solvothermal strategy, all oxygen containing groups in rGO sample were decrease significantly. This confirming effective removal of the oxygen-containing functional groups by the solvothermal reduction process [31, 32].

To study the surface characterization of GO and rGO nanosheets, FESEM was carried out at different magnifications. In Figure 3a and b, the FESEM images of GO show a wrinkled surface of GO sheets. In contrast, the surface of rGO nanosheets becomes corrugated after the solvothermal reduction process, as depicted in Figure 3c and d. Interestingly, this distinctive morphology of rGO offers more spaces for ions storage and diffusion.
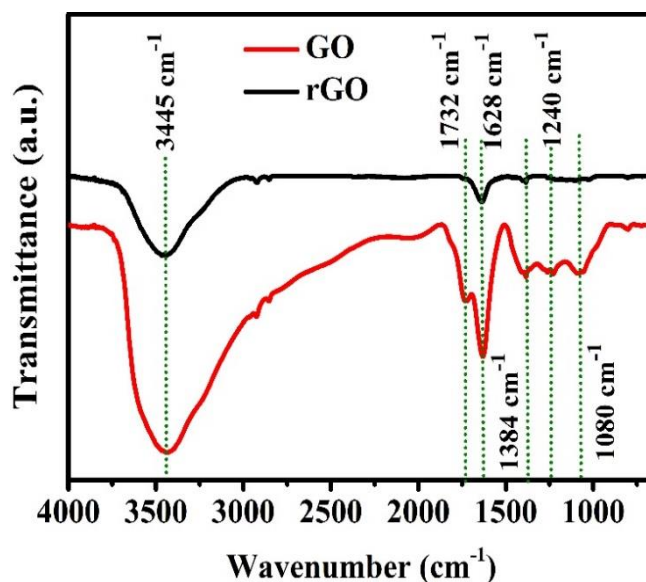
3.2 Electrochemical performance

The electrochemical behaviour of the rGO nanosheets electrode was evaluated by CV and GCD tests in the three-electrode system. Figure 4a presents the CV curves of the rGO electrode at different scan rates of a potential window range of 0 to -1 V in 5 M KOH electrolyte. All curves are rectangular-like shapes, indicating that capacitance principally originated from double-layer capacitance based on ions adsorption/desorption [33]. The existence of small anodic and cathodic peaks is ascribed to the redox pair of some active oxygen-containing functional groups on rGO nanosheets [34].

GCD was further carried out to evaluate the capacitive performance of the as-prepared rGO electrode. As shown in Figure 4b, GCD curves of rGO electrodes retained nearly linear and symmetric charge-discharge profiles which indicating the excellent capacitive behavior. Furthermore, the rGO electrode displayed no *iR* drop, indicating low internal resistance. The correlation between the specific capacitance and the different current densities is presented in Figure 5. The rGO electrode shows a specific capacitance

as high as 183 F g^{-1} at the current density of 0.25 A g^{-1}. This specific capacitance value is a better than those of rGO that it was reported previously such as green reducing agent (94 F g^{-1}) [35], chemical vapor deposition (55.3 F g^{-1}) [36], thermal exfoliation (26.1 F g^{-1}) [37] and chemical reduction (73 F g^{-1} at 1 A g^{-1}) [38].
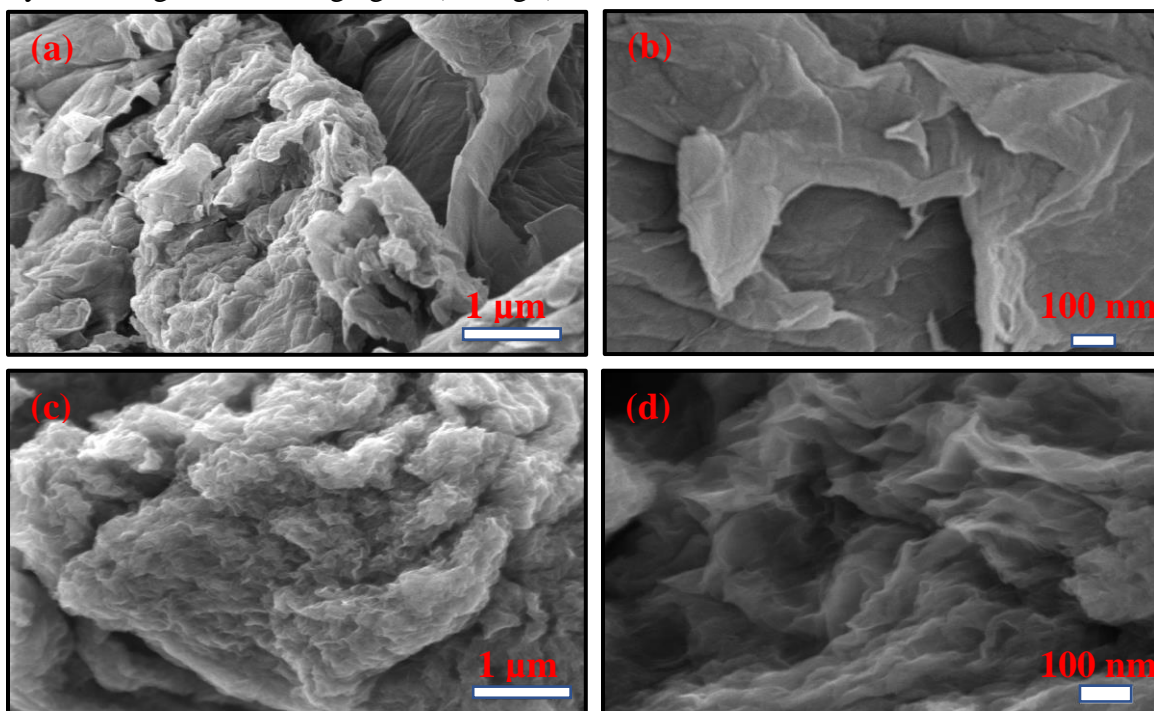

Figure 3: FESEM images of (a and b) GO and (c and d) rGO nanosheets at different resolutions.
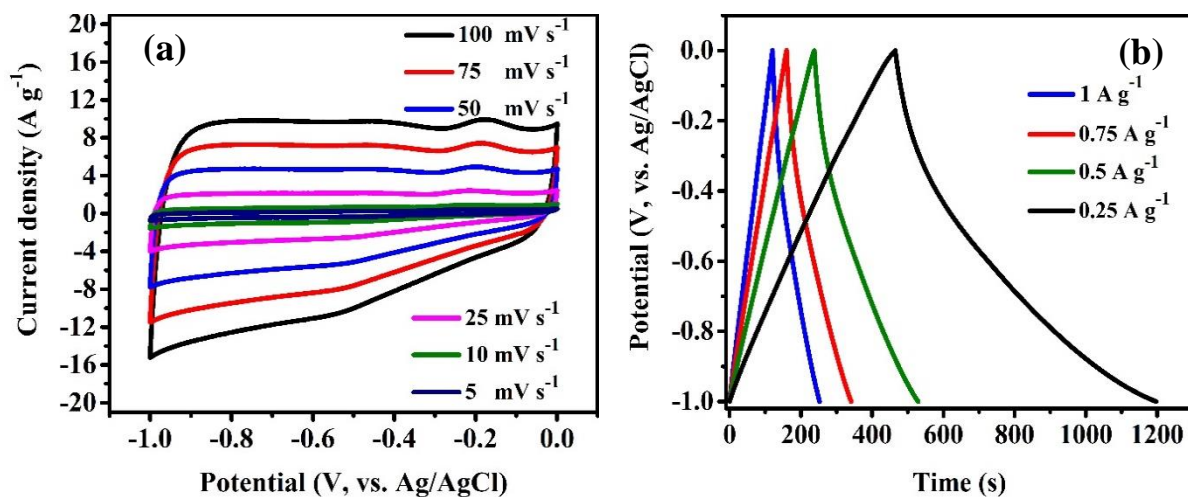

Figure 4: (a) CV and (b) GCD curves of rGO electrode at different scan rates and current densities, respectively.
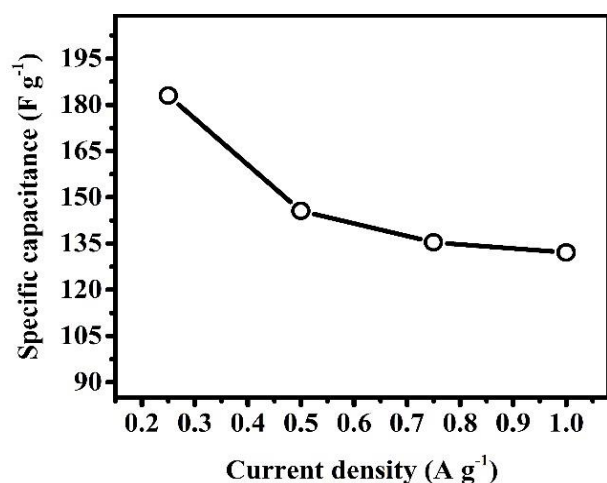
Figure 5: Specific capacitance compared to various current density for rGO electrode.

EIS test was used to study the charge kinetics of rGO electrode in KOH electrolyte. As displayed in Figure 6a, very small quasi-semicircle at the high-frequency region in Nyquist plot corresponds to the charge transfer resistance (R_{CT}), while the first intersection point at the real impedance (Z') represents the equivalent series resistance (ESR). From the inset of Figure 6a, it can be clearly seen that the low *ESR* value of rGO electrode is 430 mΩ, which attributed to the high ionic conductivity of electrolyte [39, 40]. Moreover, the rGO electrode also shows very low R_{CT} (64 mΩ), which signifies a high electrical conductivity of rGO [41].

The EIS data were further used for the evaluate the electrochemical active surface area (S_E), according to the equation reported elsewhere [42, 43]. The S_E value for rGO was calculated to be 354.5 $m^2\ g^{-1}$. The relationship of the phase angle on the frequency is illustrated in Figure 6b. The phase angle of the rGO electrode reaches -82.6°, which indicates a good capacitive performance as the ideal capacitor phase angle is -90° [44, 45]. Besides, the rGO electrode shows a flat plateau region at the low frequency, confirming again a capacitive character [46, 47].
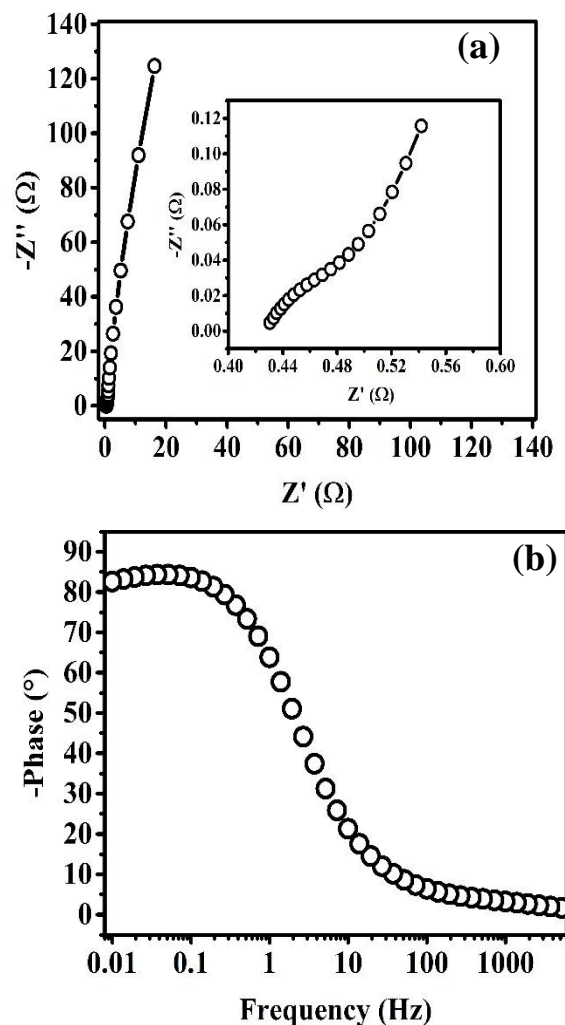

Figure 6: (a) Nyquist plot (the inset is the high-frequency region of the plot) and (b) Bode plot for rGO electrode.

Moreover, additional evaluation on the frequency response can be obtained by comparing the characteristic frequency (*f** at a phase angle of 45°) which is corresponding to the minimum time needs to discharge all the energy from the device with an efficiency of greater than 50% [48]. The relaxation time (τ) was calculated using the equation: $\tau = 1\ /\ (2\pi f^{*})$ [26]. The τ value is found to be very low (0.06 s), indicating the excellent electrochemical capacitance properties and fast charge-discharge characteristic response.

4. Conclusions

Reduced graphene oxide nanosheets are successfully synthesized by solvothermal reduction of the graphene oxide. The specific capacitance of the as-prepared rGO electrode is 183 F g^{-1} at a current density of 0.25 A g^{-1} in 5 M KOH electrolyte. Electrochemical impedance spectroscopy study of rGO nanosheets shows very small resistances and high electrochemically active surface area (354.5 m^2 g^{-1}). The finding confirms the prepared rGO is a promising electrode material for supercapacitors application.

Acknowledgements

References

[1] D. Gielen, F. Boshell, D. Saygin, M.D. Bazilian, N. Wagner, R. Gorini, The role of renewable energy in the global energy transformation, *Energy Strategy Reviews* **24** (2019) 38–50

[2] H. Chen, T.N. Cong, W. Yang, C. Tan, Y. Li, Y. Ding, Progress in electrical energy storage system: a critical review, *Progress in Natural Science* **19** (2009) 291–312.

[3] G.A.M. Ali, E.Y. Lih Teo, E.A.A. Aboelazm, H. Sadegh, A.O.H. Memar, R. Shahryari-Ghoshekandi, K.F. Chong, Capacitive performance of cysteamine functionalized carbon nanotubes, *Materials Chemistry and Physics* **197** (2017) 100–104.

[4] G.A.M. Ali, M.M. Yusoff, K.F. Chong, S.A. Makhlouf, Structural and electrochemical characteristics of graphene nanosheets as supercapacitor electrodes, *Reviews on Advanced Materials Science* **41** (2015) 35–43.

[5] Y. Wang, Y. Song, Y. Xia, Electrochemical capacitors: mechanism, materials, systems, characterization and applications, *Chemical Society Reviews* **45** (2016) 5925–5950.

[6] S. Najib, E. Erdem, Current progress achieved in novel materials for supercapacitor electrodes: mini review, *Nanoscale Advances* **1** (2019) 2817–2827.

[7] E.E. Miller, Y. Hua, F.H. Tezel, Materials for energy storage: review of electrode materials and methods of increasing capacitance for supercapacitors, *Journal of Energy Storage* **20** (2018) 30–40.

[8] D. Guo, X. Song, L. Tan, H. Ma, W. Sun, H. Pang, L. Zhang, X. Wang, A facile dissolved and reassembled strategy towards sandwich-like rGO@NiCoAl-LDHs with excellent supercapacitor performance, *Chemical Engineering Journal* **356** (2019) 955–963.

[9] G.A.M. Ali, M.M. Yusoff, K.F. Chong, Graphene: electrochemical production and its energy storage properties, *ARPN Journal of Engineering and Applied Sciences* **11** (2016) 9712–9717.

[10] M.A.A.M. Abdah, N.H.N. Azman, S. Kulandaivalu, Y. Sulaiman, Review of the use of transition-metal-oxide and conducting polymer-based fibres for high-performance supercapacitors, *Materials and Design* (2019) 108199.

[11] E.A.A. Aboelazm, Gomaa A.M. Ali, K.F. Chong, Cobalt oxide supercapacitor electrode recovered from spent lithium-ion battery, *Chemistry of Advanced Materials* **3** (2018) 67–74.

[12] H. Xia, Q. Xu, J. Zhang, Recent progress on two-dimensional nanoflake ensembles for

energy storage applications, *Nano-Micro Letters* **10** (2018) 1–30.

[13] L. Peng, P. Xiong, L. Ma, Y. Yuan, Y. Zhu, D. Chen, X. Luo, J. Lu, K. Amine, G. Yu, Holey two-dimensional transition metal oxide nanosheets for efficient energy storage, *Nature communications* **8** (2017) 1–10.

[14] Y. Sun, Q. Wu, G. Shi, Graphene based new energy materials, *Energy & Environmental Science* **4** (2011) 1113–1132.

[15] V.K. Gupta, S. Agarwal, H. Sadegh, G.A.M. Ali, A.K. Bharti, A.S. Hamdy Makhlouf, Facile route synthesis of novel graphene oxide-β-cyclodextrin nanocomposite and its application as adsorbent for removal of toxic bisphenol A from the aqueous phase, *Journal of Molecular Liquids* **237** (2017) 466–472.

[16] J. Tian, S. Wu, X. Yin, W. Wu, Novel preparation of hydrophilic graphene/graphene oxide nanosheets for supercapacitor electrode, *Applied Surface Science* **496** (2019) 143696.

[17] W. Jun, C. Bing, L. Qingqing, L. Yong, H. Ailin, L. Xiaoying, J. Qi, Preparation of reduced graphene oxide macro body and its electrochemical energy storage performance, *Colloids and Surfaces A: Physicochemical and Engineering Aspects* **582** (2019) 123859.

[18] F. Bonaccorso, A. Lombardo, T. Hasan, Z. Sun, L. Colombo, A.C. Ferrari, Production and processing of graphene and 2D crystals, *Materials Today* **15** (2012) 564–589.

[19] H. Sadegh, Development of graphene oxide from graphite: a review on synthesis, characterization and its application in wastewater treatment, *Reviews on Advanced Materials Science* **49** (2017) 38–43.

[20] K.K.H. De Silva, H.H. Huang, R.K. Joshi, M. Yoshimura, Chemical reduction of graphene oxide using green reductants, *Carbon* **119** (2017) 190–199.

[21] S. Dubin, S. Gilje, K. Wang, V.C. Tung, K. Cha, A.S. Hall, J. Farrar, R. Varshneya, Y. Yang, R.B. Kaner, A one-step, solvothermal reduction method for producing reduced graphene oxide dispersions in organic solvents, *ACS Nano* **4** (2010) 3845–3852.

[22] J. Ma, J. Wang, Y.S. He, X.Z. Liao, J. Chen, J.Z. Wang, T. Yuan, Z.F. Ma, A solvothermal strategy: one-step in situ synthesis of self-assembled 3D graphene-based composites with enhanced lithium storage capacity, *Journal of Materials Chemistry A* **2** (2014) 9200–9207.

[23] N.H. Abu Bakar, G.A.M. Ali, J. Ismail, H. Algarni, K.F. Chong, Size-dependent corrosion behavior of graphene oxide coating, *Progress in Organic Coatings* **134** (2019) 272–280.

[24] S.P. Lee, G.A.M. Ali, H. Algarni, K.F. Chong, Flake size-dependent adsorption of graphene oxide aerogel, *Journal of Molecular Liquids* **277** (2019) 175–180.

[25] M. Fahim, A. ul H.A. Shah, S. Bilal, Highly stable and efficient performance of binder-free symmetric supercapacitor fabricated with electroactive polymer synthesized *via* interfacial polymerization, *Materials* **12** (2019) 1–17.

[26] M.R. Thalji, G.A.M. Ali, H. Algarni, K.F. Chong, Al^{3+} ion intercalation pseudocapacitance study of $W_{18}O_{49}$ nanostructure, *Journal of Power Sources* **438** (2019) 227028.

[27] R.M. Zaid, F.C. Chong, E.Y.L. Teo, E.P. Ng, K.F. Chong, Reduction of graphene oxide nanosheets by natural beta carotene and its potential use as supercapacitor electrode, *Arabian Journal of Chemistry* **8** (2015) 560–569.

[28] J.L.S. Gascho, S.F. Costa, A.A.C. Recco, S.H. Pezzin, Graphene oxide films obtained by vacuum filtration: x-ray diffraction evidence of crystalline reorganization, *Journal of Nanomaterials* **2019** (2019) 12–16.

[29] S.K. Kaverlavani, S.E. Moosavifard, A. Bakouei, Designing graphene-wrapped nanoporous CuCo$_2$O$_4$ hollow spheres electrodes for high-performance asymmetric supercapacitors, *Journal of Materials Chemistry A* **5** (2017) 14301–14309.

[30] B.D. Ossonon, D. Bélanger, Synthesis and characterization of sulfophenyl-functionalized reduced graphene oxide sheets, *RSC Advances* **7** (2017) 27224–27234.

[31] M.K. Rabchinskii, A.T. Dideikin, D.A. Kirilenko, M.V. Baidakova, V.V. Shnitov, F. Roth, S.V. Konyakhin, N.A. Besedina, S.I. Pavlov, R.A. Kuricyn, N.M. Lebedeva, P.N. Brunkov, A.Y. Vul', Facile reduction of graphene oxide suspensions and films using glass wafers, *Scientific Reports* **8** (2018) 1–11.

[32] R.S. Ghoshekandi, H. Sadegh, Kinetic study of the adsorption of synthetic dyes on graphene surfaces, *Jordan Journal of chemistry* **9** (2014) 278–367.

[33] N. Guo, M. Li, X. Sun, F. Wang, R. Yang, Enzymatic hydrolysis lignin derived hierarchical porous carbon for supercapacitors in ionic liquids with high power and energy densities, *Green Chemistry* **19** (2017) 2595–2602.

[34] N. Yang, X. Xu, L. Li, H. Na, H. Wang, X. Wang, F. Xing, J. Gao, A facile method to prepare reduced graphene oxide with nano-porous structure as electrode material for high performance capacitor, *RSC Advances* **6** (2016) 42435–42442.

[35] K.S. Lau, R.T. Ginting, S.T. Tan, S.X. Chin, S. Zakaria, C.H. Chia, Sodium cholate as efficient green reducing agent for graphene oxide via flow reaction for flexible supercapacitor electrodes, *Journal of Materials Science: Materials in Electronics* **30** (2019) 19182–19188.

[36] W. Chen, Z. Fan, G. Zeng, Z. Lai, Layer-dependent supercapacitance of graphene films grown by chemical vapor deposition on nickel foam, *Journal of Power Sources* **225** (2013) 251–256.

[37] L. Buglione, E.L.K. Chng, A. Ambrosi, Z. Sofer, M. Pumera, Graphene materials preparation methods have dramatic influence upon their capacitance, *Electrochemistry Communications* **14** (2012) 5–8.

[38] W. Deng, X. Ji, M. Gómez-Mingot, F. Lu, Q. Chen, C.E. Banks, Graphene electrochemical supercapacitors: the influence of oxygen functional groups, *Chemical Communications* **48** (2012) 2770–2772.

[39] G.A.M. Ali, M.M. Yusoff, H. Algarni, K.F. Chong, One-step electrosynthesis of MnO$_2$/rGO nanocomposite and its enhanced electrochemical performance, *Ceramics International* **44** (2018) 7799–7807.

[40] B.M. Chong, N.H.N. Azman, M.A.A.M. Abdah, Y. Sulaiman, Supercapacitive performance of N-doped graphene/Mn$_3$O$_4$/Fe$_3$O$_4$ as an electrode material, *Applied Sciences* **9** (2019) 1–12.

[41] S. Zhang, J. Wu, J. Wang, W. Qiao, D. Long, L. Ling, Constructing T-Nb$_2$O$_5$@Carbon hollow core-shell nanostructures for high-rate hybrid supercapacitor, *Journal of Power Sources* **396** (2018) 88–94.

[42] G.A.M. Ali, M.M. Yusoff, E.R. Shaaban, K.F. Chong, High performance MnO$_2$ nanoflower supercapacitor electrode by electrochemical recycling of spent batteries, *Ceramics International* **43** (2017) 8440–8448.

[43] S. Chou, F. Cheng, J. Chen, Electrodeposition synthesis and electrochemical properties of nanostructured γ-MnO$_2$ films, *Journal of Power Sources* **162** (2006) 727–734.

[44] E.A.A. Aboelazm, G.A.M. Ali, H. Algarni, H. Yin, Y.L. Zhong, K.F. Chong, Magnetic electrodeposition of the hierarchical cobalt oxide nanostructure from spent lithium-ion batteries: its application as a supercapacitor electrode, *Journal of Physical Chemistry C* **122** (2018) 12200–12206.

[45] G.A.M. Ali, S. Supriya, K.F. Chong, E.R. Shaaban, H. Algarni, T. Maiyalagan, Superior supercapacitance behavior of oxygen self-doped carbon nanospheres : a conversion of Allium cepa peel to energy storage system, *Biomass Conversion and Biorefinery* (2019) 1–13.

[46] Z. Bo, W. Zhu, W. Ma, Z. Wen, X. Shuai, J. Chen, J. Yan, Z. Wang, K. Cen, X. Feng, Vertically oriented graphene bridging active-layer/current-collector interface for ultrahigh rate supercapacitors, *Advanced Materials* **25** (2013) 5799–5806.

[47] Y.H. Kwon, S. Kumar, J. Bae, Y. Seo, CVD-graphene for low equivalent series resistance in rGO/CVD-graphene/Ni-based supercapacitors, *Nanotechnology* **29** (2018).

[48] G.A.M. Ali, M.R. Thalji, W.C. Soh, H. Algarni, K.F. Chong, One-step electrochemical synthesis of MoS$_2$/graphene composite for supercapacitor application, *Journal of Solid State Electrochemistry*, (2019) 1–10.